Reaction of Organic Disulfides with Cobalt-Centered Metal Radicals. Use of the *E*- and *C*-Based Dual-Parameter Substituent Model and Quantitative Solvent Effect Analyses To Compare Outer-Sphere and Inner-Sphere Electron-Transfer Processes

Mark A. Aubart and Robert G. Bergman*

Contribution from the Department of Chemistry, University of California, Berkeley, California 94720

Received March 16, 1998

Abstract: Treatment of isolable, paramagnetic $Cp_2Ta(\mu\text{-}CH_2)_2CoCp$ (**1**, Cp = η^5-C_5H_5) with aromatic disulfides RSSR affords diamagnetic monothiolate complexes $Cp_2Ta(\mu\text{-}CH_2)_2Co(SR)Cp$ in quantitative yield. The structure of $Cp_2Ta(\mu\text{-}CH_2)_2Co(SC_6H_3(CH_3)_2)Cp$ (**2a**) has been characterized by X-ray crystallography. The mechanism of this disulfide S−S bond cleavage reaction has been probed using kinetic, substituent effect, and solvent effect techniques. A Hammett σ/ρ substituent constant analysis yields a nonlinear correlation. In contrast, application of the *E*- and *C*-based dual-parameter substituent model gives a good fit of the data and demonstrates that the reaction is sensitive to both the electrostatic and the covalent characteristics of the entering disulfide. All substituents examined (excluding *p*-(trifluoromethyl)phenyl) exhibited a solvent effect consistent with a modest amount of charge separation in the transition state. The reaction of **1** with the strongly electron withdrawing substituted bis[*p*-(trifluoromethyl)phenyl] disulfide is much more sensitive to solvent polarity changes. As a comparison system expected to proceed via a limiting outer-sphere electron-transfer mechanism, the reaction of aromatic disulfides with the 19-electron complex cobaltocene ($CoCp_2$, **3**), which leads to salts $[CoCp_2][SR]$ (**4**), was investigated using methods parallel to those employed in the study of Ta/Co complex **1**. In the cobaltocene system, the kinetic, solvent effect, and substituent effect data showed that the reaction is especially sensitive to the electrostatic character of the disulfide and relatively insensitive to its covalent character and steric bulk. The comparison of cobaltocene with Ta/Co complex **1** shows that the latter reacts with most diaryl disulfides (perhaps with the exception of *p*-CF_3 compound **2f**, which may be a borderline case) via a transition state with substantially more covalent character, and correspondingly less charge separation, than that involved in the outer-sphere reactions of Cp_2Co.

Introduction

The oxidative addition of organic disulfides to metal centers is an ubiquitous reaction in inorganic chemistry. Despite their importance in both chemistry and biology,[1−19] very little mechanistic information is available for most of these transformations. Activation of the S−S bond by coordinatively unsaturated complexes,[5,8,14,15] by 18-electron compounds with easily dissociable ligands,[11,13,16] and by homobimetallic complexes[3,4,6,10] has been observed. This last class of reactions is normally assumed to proceed via dissociation of the binuclear complex into metal radical intermediates, followed by reaction of M$^\bullet$ with the disulfide (eqs 1 and 2).

$$M{-}M \rightleftharpoons 2M^\bullet \quad (1)$$

$$2M^\bullet + RS{-}SR \rightarrow 2M{-}SR \quad (2)$$

Mechanistic study of this type of transformation has been limited to reactions in which the organometallic radicals have been generated as transient species, e.g., in the photochemical dissociation of metal−metal-bonded dimers.[3,4,6]

A clearer understanding of this process would be achieved through a thorough, direct study of the reaction of disulfides with isolable monomeric organometallic radicals.

(1) Ju, T. D.; Capps, K. B.; Lang, R. F.; Roper, G. C.; Hoff, C. D. *Inorg. Chem.* **1997**, *36*, 614.
(2) Ram, M. S.; Riordan, C. G.; Ostrander, R.; Rheingold, A. L. *Inorg. Chem.* **1995**, *34*, 5884.
(3) Abrahamson, H. B.; Freeman, M. L. *Organometallics* **1983**, *2*, 679.
(4) Abrahamson, H. B.; Freeman, M. L.; Hossain, M. B.; van der Helm, D. *Inorg. Chem.* **1984**, *23*, 2286.
(5) Aye, K.-T.; Vittal, J. J.; Puddephatt, R. J. *J. Chem. Soc., Dalton Trans.* **1993**, *12*, 1835.
(6) Brandenburg, K. L.; Heeg, M. J.; Abrahamson, H. B. *Inorg. Chem.* **1987**, *26*, 1064.
(7) Chen, D.; Ohta, N.; Ukai, M.; Masuda, M.; Yotsuyanagi, T. *Biol. Pharm. Bull.* **1994**, *17*, 1561.
(8) Collman, J. P.; Rothrock, R. K.; Stark, R. A. *Inorg. Chem.* **1977**, *16*, 437.
(9) Dedon, P. C.; Borch, R. F. *Biochem. Pharmacol.* **1987**, *36*, 1955.
(10) Goh, L. Y.; Tay, M. S. *Organometallics* **1992**, *11*, 1711.
(11) Jessop, P. G.; Rettig, S. J.; Lee, C.-L.; James, B. R. *Inorg. Chem.* **1991**, *30*, 4617.
(12) King, R. B. *J. Am. Chem. Soc.* **1963**, *85*, 1587.
(13) Lang, R. F.; Ju, T. D.; Kiss, G.; Hoff, C. D.; Bryan, J. C.; Kubas, G. J. *Inorg. Chem.* **1994**, *33*, 3899.
(14) Lang, R. F.; Ju, T. D.; Kiss, G.; Hoff, C. D.; Bryan, J. C.; Kubas, G. J. *J. Am. Chem. Soc.* **1994**, *116*, 7917.
(15) Pouly, S.; Tainturier, G.; Gautheron, B. *J. Organomet. Chem.* **1982**, *232*, C65.
(16) Recknagel, A.; Noltemeyer, M.; Stalke, D.; Pieper, U.; Schmidt, H.-G.; Edelmann, F. T. *J. Organomet. Chem.* **1991**, *411*, 347.
(17) Schollhammer, P.; Petillon, F. Y.; Pichon, R.; Poder-Guillou, S.; Talarmin, J.; Muir, K. W.; Manojlovic-Muir, L. *Organometallics* **1995**, *14*, 2277.
(18) Yotsuyanagi, T.; Ohta, N.; Futo, T.; Ito, S.; Chen, D.; Ikeda, K. *Chem. Pharm. Bull.* **1991**, *39*, 3003.
(19) Zanella, R.; Ros, R.; Graziani, M. *Inorg. Chem.* **1973**, *12*, 2736.

S0002-7863(98)00878-6 CCC: $15.00
Published on Web 08/12/1998

We previously communicated the synthesis and characterization of thiolate complexes $Cp_2Ta(\mu\text{-}CH_2)_2Co(SR)Cp$ (**2**) from the reaction of disulfides with isolable, paramagnetic $Cp_2Ta(\mu\text{-}CH_2)_2CoCp$ (**1**).[20] We also reported the preparation and isolation of $[CoCp_2][SR]$ (**4**) from the reaction of disulfides with the 19-electron complex $CoCp_2$ (**3**). This paper reports the full details of these studies and extends them to encompass the use of the *E*- and *C*-based dual-parameter substituent constant model[21] as an analytical tool for the interpretation of kinetic and substituent effect data. Additionally, we have conducted in-depth solvent effect studies on both reactions. Interpretation of these new data has shed light on the transition state of both transformations.

Results

Reaction of Aromatic Disulfides with $Cp_2Ta(\mu\text{-}CH_2)_2CoCp$ (1). Treatment of orange Co(II) complex $Cp_2Ta(\mu\text{-}CH_2)_2CoCp$ (**1**),[22] with 0.5 equiv of bis(2,6-dimethylphenyl) disulfide in methylene chloride over the course of 4 h at room temperature causes a color change to deep brown. Monitoring this reaction by ^{1}H NMR spectroscopy shows the formation of a single diamagnetic product in quantitative yield ($FeCp_2$ internal standard) with the formula $Cp_2Ta(\mu\text{-}CH_2)_2Co(SC_6H_3(CH_3)_2)Cp$ (**2a**) (eq 3). The ^{1}H NMR spectrum of **2a** in CD_2Cl_2 shows

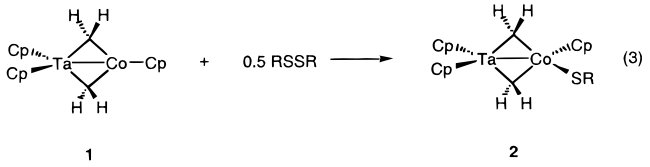

1 **2**

R =	2,6-dimethylphenyl	**2a**
	p-methoxyphenyl	**2b**
	p-tolyl	**2c**
	phenyl	**2d**
	p-chlorophenyl	**2e**
	p-trifluoromethylphenyl	**2f**

three singlets at δ 5.37, 5.04, and 4.36, indicating three inequivalent cyclopentadienyl rings along with a singlet at δ 2.43 consistent with two equivalent methyl groups on the aryl ring of the thiolate ligand. Doublet resonances at δ 8.99 and 7.39, indicative of bridging methylene units, along with a multiplet in the aromatic region make up the rest of the spectrum. Elemental analysis was also consistent with the formulation of **2a** as shown in eq 3. Dark brown platelike crystals of **2a** were obtained by toluene/pentane diffusion to give pure **2a** in 84% recrystallized yield.

To confirm the structure of **2a**, a single-crystal X-ray diffraction study was undertaken. The structure was solved by direct methods in space group $P2_12_12_1$ and refined using standard least-squares and Fourier techniques. The bonding and molecular geometry of **2a** are shown in an ORTEP diagram in Figure 1. The crystallographic data and parameters for **2a** are given in Table 1, positional parameters are given in the Supporting Information (Table S-1), and selected bond distances and angles are given in Tables 2 and 3, respectively.

There are a total of four molecules in the unit cell, and there are no abnormally short intermolecular contacts between molecules. The four-membered dimetallacycle ring is planar,

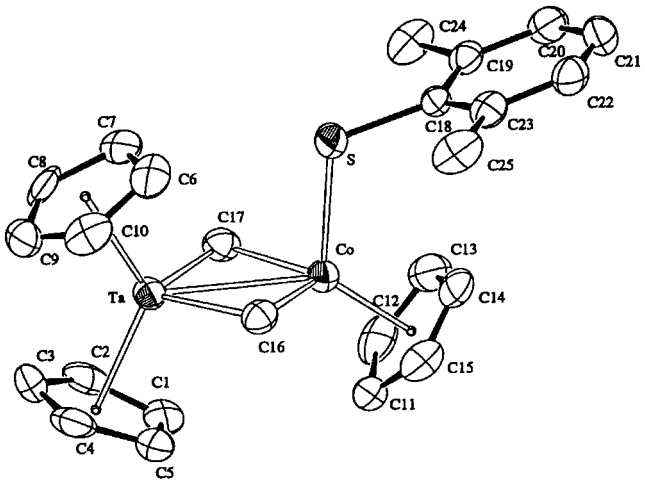

Figure 1. ORTEP diagram of $Cp_2Ta(\mu\text{-}CH_2)_2Co(SC_6H_3(CH_3)_2)Cp$ (**2a**).

Table 1. Crystal and Data Collection Parameters for $Cp_2Ta(\mu\text{-}CH_2)_2Co(SC_6H_3(CH_3)_2)Cp$ (**2a**)

formula	$TaCoSC_{25}H_{28}$
formula weight	600.44
crystal size	0.07 × 0.14 × 0.40 mm
crystal system	orthorhombic
space group	$P2_12_12_1$
a (Å)	18.8484(1)
b (Å)	9.8502(1)
c (Å)	11.2465(2)
Z	4
V (Å^3)	2088.03(7)
T (K)	153
d_{calc} (g/cm^3)	1.91
μ(Mo Kα, cm^{-1})	61.32
scan type (deg per frame)	ω (0.3)
scan rate (s per frame)	30.0
radiation	Mo Kα (λ = 0.71069 Å)
monochromator	graphite ($2\theta_{max}$ = 50.9°)
2θ Range (deg)	3.0−45.0
no. of reflns measd	9228 (unique: 2075 (R_{int} = 0.071))
R	0.042
R_w	0.058
R_{all}	0.042
GOF	3.25
p factor	0.030
no. of variables	254

Table 2. Selected Intramolecular Distances for $Cp_2Ta(\mu\text{-}CH_2)_2Co(SC_6H_3(CH_3)_2)Cp$ (**2a**)

Ta−Co	2.8005(8)	Ta−C16	2.115(6)
Ta−C17	2.126(6)	Ta−C101[a]	2.1427(2)
Ta−C102[b]	2.1220(2)	Co−S	2.317(2)
Co−C16	2.037(6)	Co−C17	2.033(6)
Co−C103[c]	1.7512(7)		

[a] C101 is the centroid of cyclopentadienyl ring C1−C5. [b] C102 is the centroid of cyclopentadienyl ring C6−C10. [c] C103 is the centroid of the cyclopentadienyl ring C11−C15.

and the Ta−Co distance of 2.8005(8) Å is approximately the sum of the atomic radii.[23] The core of the molecule is very similar to structurally characterized **1**; the two μ-CH_2−Ta distances of 2.126(6) and 2.115(6) Å in **2a** are nearly identical to those found in **1** (2.13 and 2.11 Å).[22] These distances fall roughly between those characteristic of a tantalum−carbon single bond (ca. 2.25 Å) and a tantalum−carbon double bond (ca. 2.03 Å).[24] The two μ-CH_2−Co distances of 2.037(6) and 2.033(6) Å in **2a** are also similar to those found in **1** (1.98 and

(20) Aubart, M. A.; Bergman, R. G. *J. Am. Chem. Soc.* **1996**, *118*, 1793.
(21) Drago, R. S. *Applications of Electrostatic-Covalent Models in Chemistry*; Surfside Scientific Publishers: Gainsville, FL, 1994.
(22) Goldberg, K. I.; Bergman, R. G. *J. Am. Chem. Soc.* **1988**, *110*, 4853.
(23) Slater, J. C. *J. Chem. Phys.* **1964**, *41*, 3199.
(24) Guggenberger, L. J.; Schrock, R. R. *J. Am. Chem. Soc.* **1975**, *97*, 6578.

Table 3. Selected Intramolecular Angles for $Cp_2Ta(\mu\text{-}CH_2)_2Co(SC_6H_3(CH_3)_2)Cp$ (**2a**)

Co−Ta−C101[a]	114.55(2)	Co−Ta−C102[b]	118.08(2)
C16−Ta−C17	92.6(2)	C101−Ta−C102[b]	127.32(1)
Ta−Co−S	95.28(5)	S−Co−C103[c]	122.64(5)
C16−Co−C17	97.7(2)	Ta−C16−Co	84.8(2)
Ta−C17−Co	84.6(2)	Co−S−C18	112.2(2)

[a] C101 is the centroid of cyclopentadienyl ring C1−C5. [b] C102 is the centroid of cyclopentadienyl ring C6−C10. [c] C103 is the centroid of the cyclopentadienyl ring C11−C15.

1.97 Å).[22] The Co−S distance of 2.317(2) Å is somewhat longer than in other CpCo(SR) complexes (typically 2.17−2.27 Å)[25−27] and is likely due to the steric interaction of the *o*-methyl groups with the Co-based Cp ligand. However, the Co−S distance is also approximately equal to the sum of the atomic radii.[23]

To further probe the reaction mechanism of aromatic disulfide activation by **1**, we synthesized other aryl-substituted Ta/Co thiolate complexes. $Cp_2Ta(\mu\text{-}CH_2)_2Co$(S-*p*-methoxyphenyl)Cp (**2b**), $Cp_2Ta(\mu\text{-}CH_2)_2Co$(S-*p*-tolyl)Cp (**2c**), $Cp_2Ta(\mu\text{-}CH_2)_2Co$-(S-phenyl)Cp (**2d**), $Cp_2Ta(\mu\text{-}CH_2)_2Co$(S-*p*-chlorophenyl)Cp (**2e**), and $Cp_2Ta(\mu\text{-}CH_2)_2Co$(S-*p*-(trifluoromethyl)phenyl)Cp (**2f**) were synthesized in a fashion similar to that used for the preparation of **2a**. Each compound exhibited spectral characteristics analogous to those of **2a**.

Kinetics of the Reaction of 1 with Aromatic Disulfides. Kinetic studies were carried out on the reaction of **1** with di-*p*-tolyl disulfide in methylene chloride solution using excess concentrations of the disulfide and separately with excess concentrations of the bimetallic complex. The appearance of thiolate **2c** was monitored at 15 °C by UV−vis spectroscopy, and the progress of the reaction was followed to at least greater than 3.5 half-lives. Spectra taken over time of solutions with greater than 9-fold Normal excess flooding reagent (pseudo-first-order conditions) gave a good isosbestic point at 425 nm. Conditions for the kinetic experiments are discussed in the Experimental Section. Representative kinetic data for these and other kinetics experiments are shown in the Supporting Information.

Excellent pseudo-first-order rate behavior was observed. The appearance of thiolate product **2c** under disulfide flooding conditions was monitored as a function of time at 15 °C. Pseudo-first-order rate constants were obtained by fitting the data with an exponential growth curve (alternatively, the identical rate constants could be obtained from the linear plot of the natural log of concentration vs time). The pseudo-first-order rate constants for the appearance of **2c** (k_{obs}) were plotted as a function of di-*p*-tolyl disulfide concentration under disulfide flooding conditions. A straight line was obtained that passed through the origin, indicating that the reaction is first order in both **1** and di-*p*-tolyl disulfide and second-order overall (eq 4). The second-order rate constant, k_1, obtained in this manner, was 4.3 (± 0.3) × 10^{-2} M^{-1} s^{-1}.

$$d[\mathbf{2c}]/dt = 2k_1[\mathbf{1}][\text{di-}p\text{-tolyl disulfide}] \quad (4)$$

To verify the rate law for the reaction, kinetic studies were also carried out using an excess of bimetallic complex **1**. As opposed to the standard analysis applied to the appearance of product (1 mol of **1**:1 mol of **2c**) in flooding with disulfide, the stoichiometry of the reaction requires a different derivation of the correct exponential function for flooding with **1** (0.5 mol of di-*p*-tolyl disulfide:1 mol of **2c**). This derivation, which is given in the Experimental Section, provides the correct rate constant for comparison between the two different flooding regimes. A plot of the apparent pseudo-first-order rate constants, found using the derived exponential function for the appearance of **2c**, versus the varied concentration of **1** gave a straight line that passed through the origin. The second-order rate constant k_1 found in this manner was 3.8 (± 0.3) × 10^{-2} M^{-1} s^{-1} and agrees well with the value found by flooding in disulfide.

Table 4. Rate Data for the Reaction of **1** with RSSR in CH_2Cl_2 Solvent at 15 °C

R	k_1 (M^{-1} s^{-1}, ±5%)	k^{rel}
p-$OCH_3C_6H_4$	0.132	3.5
p-$CH_3C_6H_4$	4.06 × 10^{-2}	1.1
C_6H_5	3.81 × 10^{-2}	1.0
p-ClC_6H_4	0.569	14.9
p-$CF_3C_6H_4$	0.892	23
2,6-$(CH_3)_2C_6H_3$	2.66 × 10^{-3}	0.070

The temperature dependence of the reaction rate was measured as well. The rate constant k_1 was measured for the reaction of **1** with a 20-fold Normal excess of di-*p*-tolyl disulfide for temperatures ranging from 14.9 to 45.5 °C. A linear Eyring relationship was observed (see the Supporting Information). The activation energy (E_a) for this reaction is 11.4 ± 0.2 kcal/mol, while the activation enthalpy ($\Delta H^{\ddagger}$) is 10.8 ± 0.3 kcal/mol. The activation entropy ($\Delta S^{\ddagger}$) is −27 ± 5 eu. The latter value is consistent with a reaction in which substantial translational entropy is lost in bringing the two reacting particles together in the transition state.

The effect of changing substituents on the aryl ring of the disulfides was examined. Rates were measured for the reaction of **1** with bis(*p*-methoxyphenyl), diphenyl, bis(*p*-chlorophenyl), bis[*p*-(trifluoromethyl)phenyl], and bis(2,6-dimethylphenyl) disulfide by using a 20-fold Normal excess of disulfide in methylene chloride at 15 °C (Table 4). Some of the rates were too fast to measure using standard techniques. In these cases, the reaction rate was measured using a stopped flow apparatus protected from oxygen attached to the UV−vis spectrometer (see the Experimental Section). A dramatic rate acceleration is observed in the reaction of **1** with electron-withdrawing disulfides (relative to the reaction with diphenyl disulfide), but a simple Hammett plot of the results yields a nonlinear correlation (Figure 2). Methyl substituents on the ortho positions of the aryl ring (rate constant not included in Figure 2, see Table 4) slow the reaction rate by an order of magnitude.

The rate of reaction between **1** and several of the substituted disulfides at 15 °C was measured in diethyl ether, acetone, and/or acetonitrile as well as methylene chloride solvent. The second-order rate constants, measured with a 20-fold excess of disulfide, are reported in Table 5 as rate constants relative to the parent diphenyl disulfide value in methylene chloride solvent. The rate increases by a factor of 20 in going from diethyl ether ($\epsilon = 4.3$) to acetonitrile ($\epsilon = 36.6$) for the reaction of **1** with electron-donating disulfides. For the *p*-CF_3-substituted disulfide, the rate of reaction with **1** is enhanced by a factor of 250 in going from diethyl ether to acetonitrile.

***E*- and *C*-Based Dual-Parameter Substituent Constant Correlation for the Reaction of 1 with Aromatic Disulfides.** In view of the poor correlation obtained in the simple Hammett analysis (Figure 2), the effect of changing substituents on the aryl ring of the disulfides was analyzed using the dual-parameter

(25) Bao, Q.-B.; Rheingold, A. L.; Brill, T. B. *Organometallics* **1986**, *5*, 2259.
(26) Macomber, D. W.; Rogers, R. D. *Organometallics* **1985**, *4*, 1485.
(27) Miller, E. J.; Brill, T. B.; Rheingold, A. L.; Fultz, W. C. *J. Am. Chem. Soc.* **1983**, *105*, 7580.

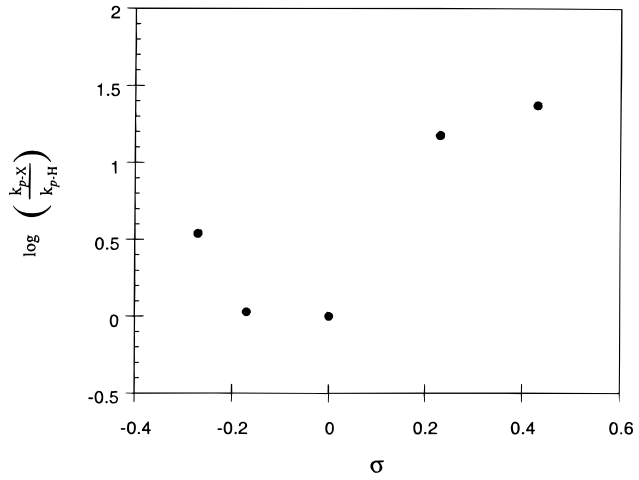

Figure 2. Hammett plot for the reaction of **1** with bis(*p*-X-phenyl) disulfides in CH_2Cl_2 solvent, where X = OCH_3, CH_3, H, Cl, or CF_3.

Table 5. Rate Data for the Reaction of **1** with RSSR at 15 °C

R	solvent[a]	k_1 ($M^{-1}s^{-1}$, ±5%)	k^{rel}
p-$OCH_3C_6H_4$	Et_2O	6.07×10^{-2}	1.6
p-$OCH_3C_6H_4$	CH_2Cl_2	0.132	3.5
p-$OCH_3C_6H_4$	$(CH_3)_2CO$	0.418	11
p-$OCH_3C_6H_4$	CH_3CN	1.33	35
p-$CH_3C_6H_4$	Et_2O	2.14×10^{-2}	0.56
p-$CH_3C_6H_4$	CH_2Cl_2	4.06×10^{-2}	1.1
p-$CH_3C_6H_4$	$(CH_3)_2CO$	0.119	3.1
p-$CH_3C_6H_4$	CH_3CN	0.377	9.9
C_6H_5	CH_2Cl_2	3.81×10^{-2}	1.0
p-ClC_6H_4	Et_2O	0.231	6.1
p-ClC_6H_4	CH_2Cl_2	0.569	14.9
p-ClC_6H_4	$(CH_3)_2CO$	1.62	43
p-$CF_3C_6H_4$	Et_2O	0.280	7.3
p-$CF_3C_6H_4$	CH_2Cl_2	0.892	23
p-$CF_3C_6H_4$	$(CH_3)_2CO$	25.6	672
p-$CF_3C_6H_4$	CH_3CN	69.7	1829

[a] Solvent (dielectric constant ϵ): Et_2O (4.3), CH_2Cl_2 (8.9), $(CH_3)_2CO$ (20.7), CH_3CN (36.6).

substituent constant equation shown in eq 5 .[28] This method

$$\Delta\chi^X = d^E\Delta E^X + d^C\Delta C^X + \Delta\chi^H \quad (5)$$

of analysis has been developed by Drago in studies of other reactions.[21,29−32] The ΔE^X and ΔC^X parameters are the dual-parameter analogues (electrostatic and covalent, respectively) of the more familiar Hammett substituent constant σ. Likewise, the d^E and d^C parameters are described as the separation of the analogous ρ value, split into an electrostatic contribution and a covalent contribution, respectively. The value of the measured property (in this case, the second-order rate constant) for an X substituent is symbolized by $\Delta\chi^X$, while the second-order rate constant for diphenyl disulfide (X = H) is symbolized by $\Delta\chi^H$.

From the known[29] values of ΔE^X and ΔC^X for para substituents X = OCH_3, CH_3, H, Cl, and CF_3 and the corresponding measured rate constants, a series of equations having the form of eq 5 can be expressed. After least-squares minimization of these equations, values for d^E, d^C, and $\Delta\chi^H$ were obtained for diethyl ether (four equations), methylene chloride (five equations), and acetone (four equations). Values for d^E and d^C are shown in Table 6. An example of the quality of fit for the reaction of **1** with diaryl disulfides in acetone is demonstrated in Table 7. The log of the measured rate constant is compared with the log of the calculated rate constant from the data analysis. (Fits of poorer quality were obtained for diethyl ether and methylene chloride solvents but reflect the same trend, vide infra.)[33]

Table 6. Calculated Values of d^E and d^C for the Reaction of **1** with Bis(*p*-X-phenyl) Disulfides in Different Solvents

solvent	d^E	d^C	d^E/d^C
Et_2O	−7.65	0.94	−8.1
$(CH_3)_2CO$	−27.6	5.29	−5.2
CH_2Cl_2	−17.0	3.21	−5.3

Table 7. Measured ($(CH_3)_2CO$ Solvent, 15 °C) and Calculated Rate Constants for the Reaction of **1** with Bis(*p*-X-phenyl) Disulfides

X	log k_{measd}	log k_{calcd}
OCH_3	−0.379	−0.378
CH_3	−0.923	−0.925
H	0.210	0.212
CF_3	1.41	1.41

Because of the relatively small ratio d^E/d^C in all cases, either the electrostatic *or* the covalent component of the reaction can be the dominant influence on the reaction rate, depending on the electrostatic and covalent characteristics of the substituent. An analogous duality has been observed in the evaluation of the ionization energies for a series of monosubstituted benzene chromium tricarbonyl complexes ($d^E/d^C = 1.97$, $d^E = -0.59$, $d^C = -0.30$).[21] Similar values for d^E and d^C indicate that the measured property is sensitive to *both* the electrostatic and covalent character of the substituent.

Quantitative Solvent Effect Analysis for the Reaction of 1 with Aromatic Disulfides Using a Unified Solvation Model (USM). Drago has devised an approach to the quantitative evaluation of solvent effects that divides solvents into two general groups. The first group is capable of *specific* donor−acceptor solvent−solute interactions (e.g., hydrogen bonding, cation-π interactions, etc.), and the second group is characterized only by *nonspecific* solvent−solute interactions. In examining solvent effects on the reaction of **1** with substituted diaryl disulfides, we restricted our investigation to solvents from the second group, so that the reaction rates could be analyzed using the USM-derived correlation for nonspecific solvation shown in eq 6 .[21,34,35] The S' value is a measure of a solvent's polarity

$$\Delta\chi = PS' + W \quad (6)$$

and has been derived using a variety of spectroscopic transitions that are independent of specific solute−solvent interactions. The value of the measured property (in this case, the second-order rate constant) is symbolized by $\Delta\chi$, while P represents the sensitivity of the system studied to solvent polarity. If the solvation phenomenon is nonspecific for a given system, a linear correlation between $\Delta\chi$ and S' with intercept W is anticipated. The intercept is the value of $\Delta\chi$ in the absence of solvent.

Plots of the log of the second-order rate constants for the reaction of **1** with disulfides versus the known S' values for

(28) Another useful method of analysis, the correlation of log k to the electronic parameter χ, has been developed by Giering and co-workers (see, for example: Bartholomew, J.; Fernandez, A. L.; Lorsbach, B. A.; Wilson, M. R.; Prock, A.; Giering, W. P. *Organometallics* **1996**, *15*, 295). In our case, this analysis did not yield much insight beyond the Hammett analysis.

(29) Drago, R. S.; Dadmun, A. P. *J. Am. Chem. Soc.* **1994**, *116*, 1792.

(30) Drago, R. S. *Organometallics* **1995**, *14*, 3408.

(31) Drago, R. S. *Inorg. Chem.* **1995**, *34*, 3543 and references therein.

(32) Drago, R. S. *J. Organomet. Chem.* **1996**, *512*, 61.

(33) R^2 values for these fits ranged from 0.9999 to 0.82; however, similar trends were observed between fits of varying qualities.

(34) Drago, R. S.; Ferris, D. C. *J. Phys. Chem.* **1995**, *99*, 6563.

(35) Drago, R. S. *J. Chem. Soc., Perkin Trans. 2* **1992**, 1827.

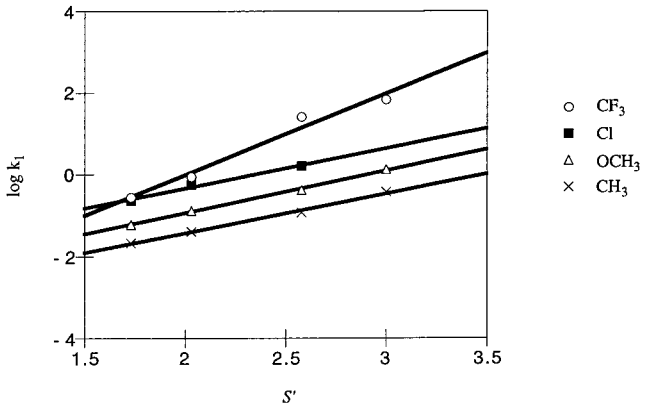

Figure 3. Nonspecific solvation plots of log k_1 vs S' for the reaction of **1** with bis(*p*-X-phenyl) disulfides, where X = OCH_3, CH_3, Cl, or CF_3. Values for *P* and *W* are shown in Table 8.

Table 8. Solvent Effect Analysis Results for the Reaction of **1** with RSSR at 15 °C

R	*P*	*W*
p-$OCH_3C_6H_4$	1.03	−3.0
p-$CH_3C_6H_4$	0.96	−3.4
p-ClC_6H_4	0.97	−2.3
p-$CF_3C_6H_4$	1.99	−4.0

diethyl ether (1.73), methylene chloride (2.03), acetone (2.58), and acetonitrile (3.00) produced the straight lines shown in Figure 3. The *P* and *W* values are reported in Table 8. The responses of the reaction of **1** with bis(*p*-X-phenyl) disulfides to solvent polarity are approximately the same for X = OCH_3, CH_3, and Cl. The significant increase in *P* for the reaction of **1** with bis[*p*-(trifluoromethyl)phenyl] disulfide suggests that more charge separation in the transition state is necessary with this substrate. However, the *W* values, admittedly an extrapolation, appear to indicate that in the absence of solvent about the same rate is observed regardless of substituent.

Reaction of Aromatic Disulfides with $CoCp_2$ (3). Cobaltocene ($CoCp_2$, **3**), having a well-shielded metal center and a high reduction potential, is a well-known outer sphere one-electron donor. To provide a limiting outer sphere metal + disulfide reaction to compare with the **1** + disulfide transformation, we examined the reaction of **3** with diaryl disulfides. Treatment of black **3** with 0.5 equiv of bis[*p*-(trifluoromethyl)-phenyl] disulfide at room temperature in acetonitrile immediately causes a color change to orange. Monitoring this reaction by ^{1}H NMR spectroscopy shows the formation of a single diamagnetic product in quantitative yield ($FeCp_2$ internal standard) with the formula [$CoCp_2$][S-*p*-(trifluoromethyl)phenyl] (**4a**) (eq 7).

$$\underset{\mathbf{3}}{CoCp_2} + 0.5\ RSSR \xrightarrow{15\ °C} \underset{\mathbf{4}}{[CoCp_2][SR]} \qquad (7)$$

R =	*p*-trifluoromethylphenyl	**4a**
	p-chlorophenyl	**4b**
	phenyl	**4c**
	p-tolyl	**4d**
	p-methoxyphenyl	**4e**
	2,6-dimethylphenyl	**4f**

The ^{1}H NMR spectrum of **4a** in CD_3CN shows a singlet at δ 5.64, indicative of two equivalent cyclopentadienyl rings, along with two aromatic resonances. Elemental analysis was also consistent with the formulation of **4a** as shown in eq 7. Bright orange needlelike crystals of **4a** were obtained by layering an acetonitrile solution with diethyl ether and allowing the solvents to diffuse. Pure **4a** was obtained in 87% recrystallized yield. The other cobaltocenium salts **4b**−**f** were characterized by NMR spectroscopy; their spectra were similar to that of **4a**.

Table 9. Rate Data for the Reaction of **3** with RSSR at 15 °C

R	solvent[a]	k_1 (M^{-1} s^{-1}, ±10%)	k^{rel}
p-$CF_3C_6H_4$	CH_2Cl_2	0.32	2.9×10^2
p-$CF_3C_6H_4$	$(CH_3)_2CO$	34	3.1×10^4
p-$CF_3C_6H_4$	CH_3CN	1.8×10^3	1.6×10^6
p-ClC_6H_4	CH_2Cl_2	1.9×10^{-2}	17
C_6H_5	CH_2Cl_2	1.1×10^{-3}	1.0
p-$CH_3C_6H_4$	CH_2Cl_2	4.8×10^{-4}	0.44
p-$CH_3C_6H_4$	$(CH_3)_2CO$	4.0×10^{-3}	3.6
p-$CH_3C_6H_4$	CH_3CN	5.2×10^{-2}	47
p-$OCH_3C_6H_4$	CH_2Cl_2	4.3×10^{-4}	0.39
2,6-$(CH_3)_2C_6H_3$	CH_2Cl_2	9.7×10^{-4}	0.88

[a] Solvent (dielectric constant ϵ): CH_2Cl_2 (8.9), $(CH_3)_2CO$ (20.7), CH_3CN (36.6).

Kinetics of the Reaction of 3 with Aromatic Disulfides. Kinetic studies were carried out under conditions identical to those used in the reaction of **1** with disulfides except that only the disulfide flooding regime was investigated. The disappearance of **3** was monitored at 15 °C by UV−vis spectroscopy, and the progress of the reaction was followed to at least greater than 3.5 half-lives. Spectra taken over time of solutions with greater than 9-fold Normal excess disulfide (pseudo-first-order conditions) gave a good isosbestic point at 435 nm. Conditions for the kinetic experiments are discussed in the Experimental Section.

Excellent pseudo-first-order behavior, consistent with the rate law shown in eq 8, was observed.

$$-d[\mathbf{3}]/dt = 2k_1[\mathbf{3}][RSSR] \qquad (8)$$

The disappearance of **3** under di-*p*-tolyl disulfide flooding conditions was monitored as a function of time at 15 °C. Pseudo-first-order rate constants were obtained as in the reaction of **1** with disulfides, with the exception that an exponential decay function was fit instead of a growth function.

The results of changing aryl substituents and solvents in the reaction with **3** are shown in Table 9. Rates were measured for the reaction of **3** with bis[*p*-(trifluoromethyl)phenyl], bis-(*p*-chlorophenyl), diphenyl, di-*p*-tolyl, bis(*p*-methoxyphenyl), and bis(2,6-dimethylphenyl) disulfide. In contrast to the behavior of **1** discussed above, a simple Hammett plot yields a fairly linear correlation (Figure 4) for the reaction of di-*p*-substituted phenyl disulfides with **3**. This plot should be interpreted with care due to the large error associated with the rate constants, but it does distinctly show that the reaction rate increases in going from electron-donating substituents to electron-withdrawing substituents ($\rho = 4.2$). Also, in contrast to **1**, methyl substituents on the ortho positions of the aryl ring do not slow the reaction of **3** with bis(2,6-dimethylphenyl) disulfide.

The rates of reaction between **3** and di-*p*-tolyl disulfide, and **3** and bis[*p*-(trifluoromethyl)phenyl] disulfide, were measured at 15 °C in acetone and acetonitrile as well as in methylene chloride solvent. The second-order rate constants, measured with a 20-fold excess of disulfide, are reported in Table 9 as rate constants relative to the parent diphenyl disulfide value in

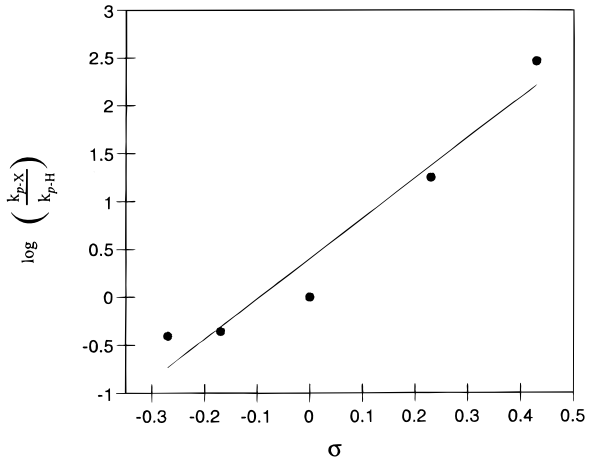

Figure 4. Hammett plot for the reaction of **3** with bis(*p*-X-phenyl) disulfides in CH_2Cl_2 solvent, where X = OCH_3, CH_3, H, Cl, or CF_3 (ρ = 4.2).

Table 10. Measured (CH_2Cl_2 Solvent, 15 °C) and Calculated Rate Constants for the Reaction of **3** with Bis(*p*-X-phenyl) Disulfides

X	log k_{measd}	log k_{calcd}
CF_3	−0.49	−0.52
Cl	−1.7	−1.7
H	−3.0	−2.8
CH_3	−3.3	−3.5
OCH_3	−3.4	−3.3

methylene chloride solvent. The rate increases by 2 orders of magnitude in going from methylene chloride (ϵ = 8.9) to acetonitrile (ϵ = 36.6) for the reaction of **3** with di-*p*-tolyl disulfide, while for the same solvents the enhancement is 3 orders of magnitude for the reaction of **3** with the *p*-CF_3-substituted disulfide.

***E*- and *C*-Based Dual-Parameter Substituent Constant Correlation for the Reaction of 3 with Aromatic Disulfides.** The effect of changing substituents on the aryl ring of the disulfides was analyzed using the method described (vide supra) for the reaction of **1** with disulfides in methylene chloride solvent. After least-squares minimization, values for d^E (−16.2) and d^C (1.00) were obtained. A measure of the fit is demonstrated in Table 10 where the log of the measured rate constant is compared with the log of the calculated rate constant from the data analysis. The ratio d^E/d^C (−16.2) for the reaction of **3** with disulfides is quite different from that measured for Ta/Co complex **1** but is approximately the same as the ratio d^E/d^C for the dissociation of *p*-substituted benzoic acids (16.3).[21] This relatively large difference between d^E and d^C indicates that both the benzoic acid dissociation and the **3** + disulfide reactions are relatively insensitive to the covalent character of the substituent compared to the electrostatic component. This interpretation is consistent with the good Hammett correlation and the expected reactivity of paramagnetic **3**.

Quantitative Solvent Effect Analysis for the Reaction of 3 with Aromatic Disulfides Using a Unified Solvation Model. The effect of nonspecific solvents on the rate of reaction of **3** with substituted diaryl disulfides was analyzed using the method described (vide supra) for the reaction of **1** with disulfides. Plots of the log of the second-order rate constants versus the known S' values for methylene chloride (2.03), acetone (2.58), and acetonitrile (3.00) produced the straight lines shown in Figure 5. The *P* and *W* values for the reaction of **3** with di-*p*-tolyl disulfide and with bis[*p*-(trifluoromethyl)phenyl] disulfide are 2.04 and −7.5 and 3.89 and −8.4, respectively. The large

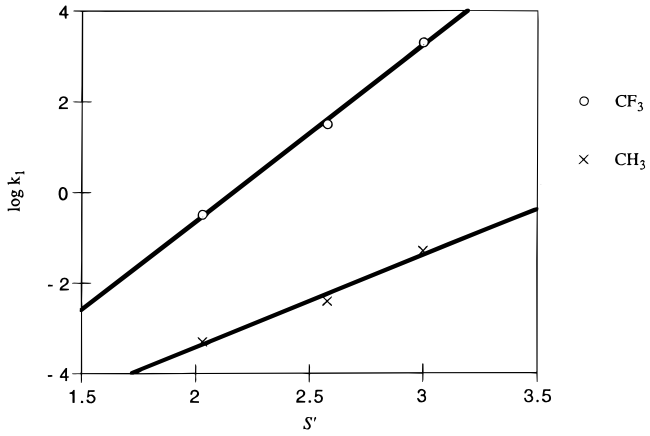

Figure 5. Nonspecific solvation plots of log k_1 vs S' for the reaction of **3** with bis(*p*-X-phenyl) disulfides, where X = CH_3 (P = 2.04, W = −7.5) or CF_3 (P = 3.89, w = −8.4).

Table 11. Peak Potentials for RSSR Measured Using Square Wave Voltammetry (vs 0.01 M $Ag/AgNO_3$)

R	E_p (± 0.03 V)	R	E_p (± 0.03 V)
p-$OCH_3C_6H_4$	−2.30	*p*-ClC_6H_4	−1.93
p-$CH_3C_6H_4$	−2.26	*p*-$CF_3C_6H_4$	−1.87
C_6H_5	−2.18		

values of P for both reactions relative to the reaction of **1** with electron-donating substituted disulfides suggest that this transformation requires significant charge separation in the transition state. The reaction of **3** with bis[*p*-(trifluoromethyl)phenyl] disulfide is much more sensitive to solvent polarity than the reaction of **3** with the *p*-methyl-substituted disulfide. This appears to represent a development of even more charge buildup in the transition state with this substituent. Again, the extrapolated W values appear to indicate that in the absence of solvent, about the same rate is observed regardless of substituent. In comparison to the reaction of **1** with disulfides, the W values are more negative consistent with a slower rate in the absence of solvent for the reaction of **3**.

Electrochemistry. To better understand and confirm the role that electron transfer plays in these reactions, an attempt to measure the reduction potentials for the substituted diaryl disulfides was made using square wave voltammetry. The electrochemical reduction of diaryl disulfides has been studied extensively and is known to be irreversible;[36] this was confirmed in our experiments. However, we felt it would be useful to determine qualitatively whether electrochemical reduction of the substituted diaryl disulfides correlated with the rates of their reactions with **1** and **3**. To make this assessment, we measured the peak potentials of the disulfides under identical square wave voltammetry[37] conditions (see the Experimental Section for details). These values (relative to 0.01 M $Ag/AgNO_3$, see Table 11) correlate linearly with the Hammett parameter σ, suggesting that the irreversible potentials provide at least a reasonable approximation to the reversible ones. To assess whether the measured potentials and the **1** + RSSR and **3** + RSSR rates follow the type of Marcus relationship[38,39] that would be expected for an outer-sphere electron-transfer process, the log of the rate constants were plotted against the potentials. As

(36) Liu, M.; Visco, S. J.; De Jonghe, L. C. *J. Electrochem. Soc.* **1989**, *136*, 2570.
(37) Osteryoung, J.; O'Dea, J. J. In *Electroanalytical Chemistry*; Bard, A. J., Ed.; Marcel Dekker: New York, 1987; Vol. 14; pp 209−309.
(38) Eberson, L. *Electron-Transfer Reactions in Organic Chemistry*; Springer-Verlag: Berlin, 1987.
(39) Marcus, R. A. *Annu. Rev. Phys. Chem.* **1964**, *15*, 155.

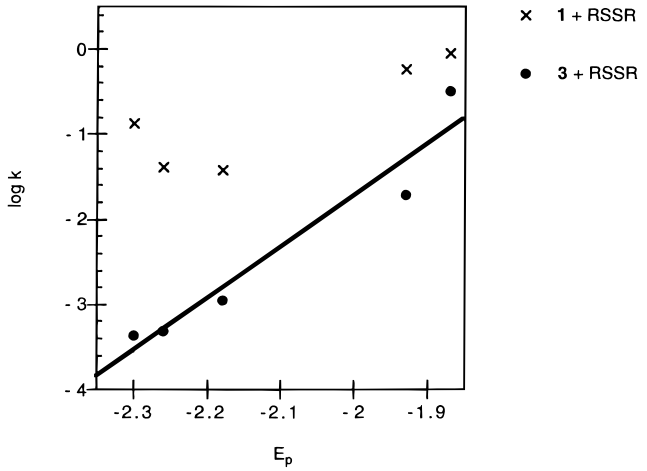

Figure 6. Qualitative Marcus plots of log k_1 vs E_p for the reaction of **1** and **3** with bis(*p*-X-phenyl) disulfides.

Scheme 1

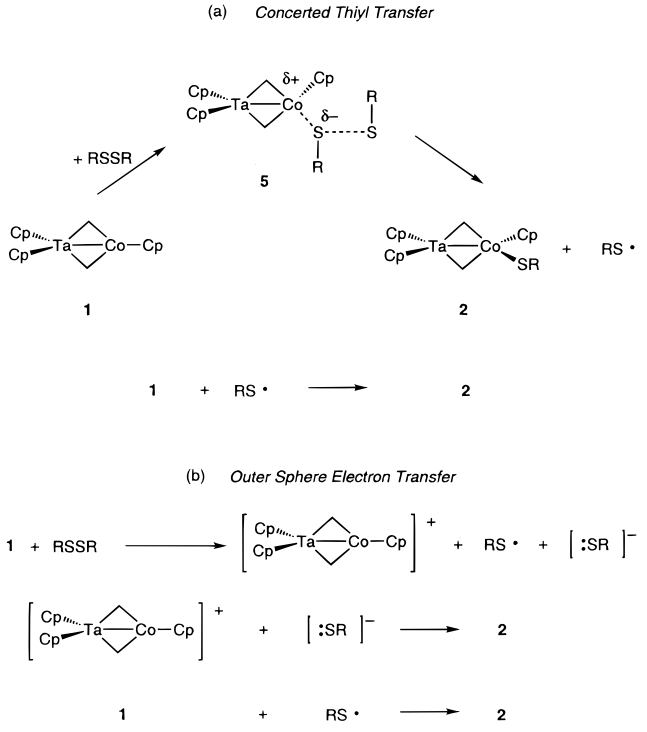

can be seen in Figure 6, a reasonable correlation is observed for the reaction of $CoCp_2$ with disulfides, while the correlation in the Ta/Co complex **1** case is very poor.

Discussion

Mechanism of the Reaction of $Cp_2Ta(\mu\text{-}CH_2)_2CoCp$ (1) with Aromatic Disulfides. Outlined in Scheme 1 are two possible mechanistic pathways for the reaction of $Cp_2Ta(\mu\text{-}CH_2)_2CoCp$ (**1**) with disulfides that are consistent with the rate law that is observed. Possibility (a) involves a rate-determining direct attack of the cobalt center at sulfur. In a concerted fashion, disulfide cleavage is achieved simultaneously with thiolate bond formation. This is followed by rapid reaction of the generated thiyl radical with a second mole of **1**. Possibility (b) involves a discrete, outer-sphere electron-transfer from the cobalt center to the disulfide. Rapid dissociation of the disulfide radical anion leads to a cationic Ta/Co intermediate along with a thiyl radical and a thiolate anion. Finally, fast collapse of the ion pair and fast reaction of **1** with thiyl radical leads to 2 mol of product. These paths differ in the timing of disulfide bond cleavage and Co−thiolate bond formation and in the amount of charge that builds up in the transition state.

Table 12. Products $d^E\Delta E^X$ and $d^C\Delta C^X$ for the Reaction of **1** with Bis(*p*-X-phenyl) Disulfides and the Reaction of **3** with Bis(*p*-X-phenyl) Disulfides in CH_2Cl_2 Solvent

X	ΔE^X [a]	ΔC^X [a]	$d^E\Delta E^X, d^C\Delta C^X$ (**1** + RSSR)	$d^E\Delta E^X, d^C\Delta C^X$ (**3** + RSSR)
OCH_3	0.048	0.285	−0.82, 0.91	−0.78, 0.29
CH_3	0.05	0.192	−0.85, 0.62	−0.81, 0.19
H	0	0	0.00, 0.00	0.00, 0.00
Cl	−0.09	−0.323	1.53, −1.04	1.46, −0.32
CF_3	−0.176	−0.545	2.99, −1.75	2.85, −0.55

[a] From ref 31.

To distinguish these two mechanisms, we began by examining the effect of different substituents on the phenyl ring of the disulfide in the reaction in CH_2Cl_2 solvent. The large steric effect observed on the reaction of **1** with bis(2,6-dimethylphenyl) disulfide (a 15-fold rate decrease relative to the reaction of **1** with di-*p*-tolyl disulfide) implies a tight transition state. This suggests that the entering disulfide must encounter the cobalt center at close range and argues for a concerted process such as the one shown in pathway (a). The absence of a correlation between the log of the relative rate constants versus the disulfide reduction potentials also supports the proposal of an inner-sphere process. However, contrary to a purely covalent thiyl transfer pathway, both electron-donating and electron-withdrawing groups enhanced the reaction rate. This can be seen by examination of the Hammett plot (Figure 2) which clearly shows a nonlinear correlation.

Drago has made a case that the use of single parameter, organic-based substituent scales such as the Hammett correlation have met with limited success in interpreting reactivity in some organic and organometallic systems.[31] To solve this problem, he has proposed the use of a dual-parameter substituent model which separates electrostatic from covalent contributions to the rate; the derivation of this model has been published elsewhere.[21] The basis for applying Drago's *E*- and *C*-based model is shown in eq 5, where d^E and d^C can be described as the separation of the Hammett ρ value into an electrostatic (*E*) contribution and a covalent (*C*) contribution, respectively. Interpretation of these values can provide insight into reactions in which a single-parameter approach is insufficient.[40]

In the case of the reaction of **1** with bis(*p*-X-phenyl) disulfides, the dual parameter approach was applied. Drago's values of ΔE^X and ΔC^X, derived from well-established reactions, indicate the proportional effect that a substituent can have on a reaction system. For example, a positive ΔE^X group will enhance the rate of a reaction in which d^E is positive. Conversely, if d^E is negative, the positive ΔE^X substituent will retard the reaction rate. Thus, to evaluate d^E and d^C, the independent *sensitivities* of our particular reaction to the *E* and *C* characteristics of the substituents, the products $d^E\Delta E^X$ and $d^C\Delta C^X$ are calculated to see which term dominates. The results of these calculations for the reaction in methylene chloride solvent are shown in Table 12 and illustrated in Figure 7. The bar graph is a direct plot of eq 5. For a given substituent, the sum of the electrostatic contribution, covalent contribution, and log of the diphenyl disulfide rate constant makes up the overall

(40) The use of multiparameter linear free energy relationships has a long history. See, for example: Lowry, T. H.; Richardson, K. S. *Mechanism and Theory in Organic Chemistry*, 3rd ed.; HarperCollins Publishers: New York, 1987; pp 155−159.

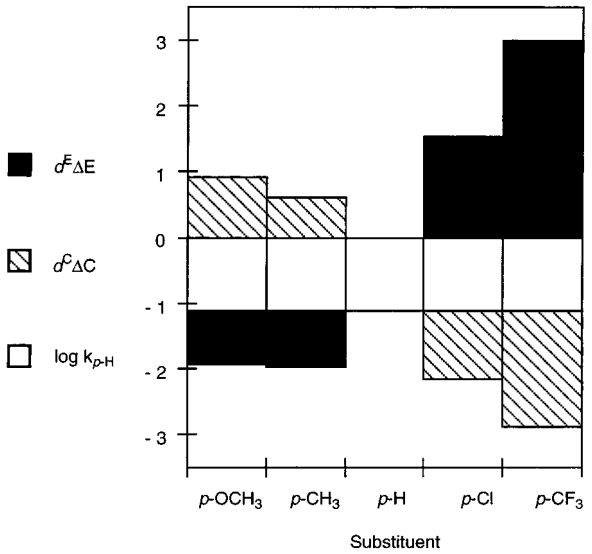

Figure 7. Graphical presentation of eq 5 for the reaction of **1** with disulfides, showing the contribution of electrostatic and covalent effects (relative to diphenyl disulfide) toward the overall rate constant. Adding the three regions for each disulfide gives the overall rate constant for that system.

relative rate constant. For the strongly electron-withdrawing group *p*-trifluoromethyl, the electrostatic contribution ($d^E\Delta E^X$) dominates. Because it is positive, the reaction rate is enhanced by the electrostatic term much more than it is retarded by the negative covalent component. The dominant term in the case of the electron-donating *p*-methoxy substituent is the covalent term ($d^C\Delta C^X$) which increases the reaction rate slightly more than the electrostatic character decreases it. The small magnitude of the sums of $d^E\Delta E^X$ and $d^C\Delta C^X$ in the case of all the para substituents except for trifluoromethyl illustrate the close balance of electrostatic and covalent characteristics of the transition state in these cases.

With this information in hand, we now turn to the effect of solvent on the reaction of **1** with substituted disulfides. The data were analyzed using a nonspecific solvation model proposed by Drago. The unified solvation model (USM) was used to derive empirical values for solvent polarity, S'. Drago's derivation relies on data from a wide variety of spectral transitions of solutes in varying solvents and has been reported elsewhere.[35] The basis for this derivation is shown in eq 6, where P is the sensitivity of the measured property to solvent polarity. An advantage of this analysis is that a concrete value for comparison with other systems is obtained.

In the case of the reaction of **1** with bis(*p*-X-phenyl) disulfides, the P values obtained indicate how sensitive the reaction is to solvent polarity change. For example, a large positive P indicates a transition state in which a polar solvent causes a large increase in rate, leading to the conclusion that a significant degree of charge separation develops in the transition state. However, in the reaction of Ta/Co complex **1** with all the substituted disulfides examined except for bis[*p*-(trifluoromethyl)phenyl] disulfide, the P value is approximately 1.0. This indicates that for these reactions only a modest amount of charge is built up in the transition state.[41] In contrast, the P value for the reaction of **1** with the *p*-CF_3-substituted disulfide is significantly greater (2.0). This indicates that there is more charge separation in the transition state for the reaction of **1** with bis[*p*-(trifluoromethyl)phenyl] disulfide than there is for the reaction of **1** with other disulfides.

(41) Another interpretation could be that charges develop in the ground state of the starting materials, but this seems unlikely.

Scheme 2

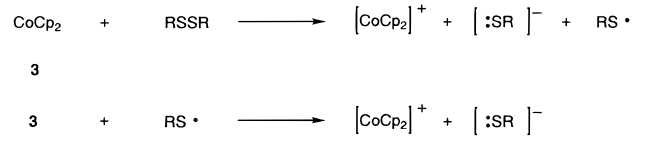

The combination of effects found by these analyses can be explained by transition structure **5** shown in Scheme 1. The amount of charge buildup in the transition state varies with the electrostatic and covalent character of the incoming disulfide. In the case of most substituents (excluding *p*-CF_3) the amount of separated charge is modest in the transition state. Neither electrostatic or covalent contributions are important enough to force the system to be very sensitive to solvent polarity change. In the case of the *p*-CF_3 substituent, the amount of charge buildup begins to approach that of pathway (b) shown in Scheme 1. The electrostatic contribution to the overall rate dominates completely, and the reaction becomes much more sensitive to solvent polarity change. Thus, the good fit to the *E*- and *C*-based model suggests that there is continuum between the two mechanistic extremes shown in Scheme 1.

Mechanism of the Reaction of $CoCp_2$ (3) with Aromatic Disulfides. The reaction of 19-electron complex $CoCp_2$ (**3**) with disulfides was expected to occur via an outer-sphere single-electron-transfer pathway. This process is depicted in Scheme 2. Transfer of an electron from the cobalt center to the disulfide generates the disulfide radical anion, and then rapid dissociation of this anion results in the formation of a thiyl radical and a thiolate anion. The thiolate associates with the cationic cobalt center to yield 1 mol of product **4**. The resulting thiyl radical can then combine with another 1 mol of **3** to give an additional 1 mol of **4**. We hoped that this simpler mechanistic situation could be used as a benchmark (i.e., closer to pure *E*) system to compare with the reaction of **1** with disulfides.

The kinetic, substituent effect, and solvent effect studies on the reaction of **3** with disulfides indicated that an outer-sphere mechanism was operative. Perhaps most convincing with respect to the reaction of **1** with disulfides was the lack of a steric effect in the reaction of **3** with bis(2,6-dimethylphenyl) disulfide. In contrast to the situation with **1**, the reaction of **3** with disulfides exhibited a good Hammett correlation (Figure 4), showing that electron-donating substituents hamper the reaction rate while electron-withdrawing substituents enhance it. The linear Marcus correlation observed for the **3** + disulfides transformation (Figure 5) also supports the proposal of an outer-sphere mechanism.

To use the reaction of **3** with disulfides as a comparative tool in examining the reaction of **1** with disulfides, the *E*- and *C*-based dual-parameter substituent constant analysis was applied here also. Again to evaluate the values for d^E and d^C, the products $d^E\Delta E^X$ and $d^C\Delta C^X$ are calculated to see which term dominates. The results of these calculations are shown in Table 12 and illustrated in Figure 8. In the case of every substituent examined here, the electrostatic contribution was the dominant component in the rate. In the case of the electron-withdrawing substituent *p*-trifluoromethyl, this means that the reaction rate is enhanced by the electrostatic component (dominant, positive $d^E\Delta E^X$) much more than it is decreased by the covalent character (negative $d^C\Delta C^X$). In the case of electron-donating substituents, the effect of the electrostatic character is reversed. The reaction rate is hampered by the electrostatic component (dominant, negative $d^C\Delta C^X$) more than it is increased by the covalent

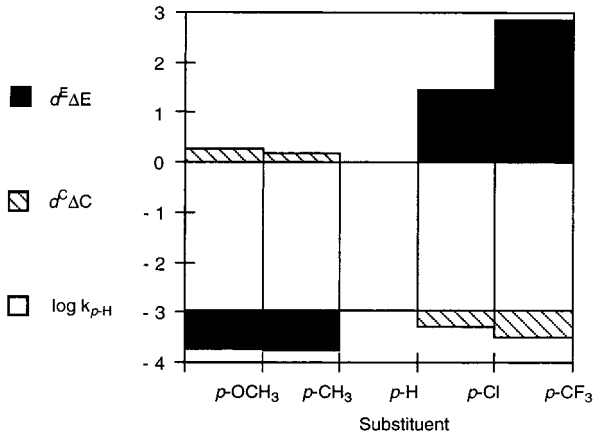

Figure 8. Graphical presentation of eq 5 for the reaction of **3** with disulfides, showing the contribution of electrostatic and covalent effects (relative to diphenyl disulfide) toward the overall rate constant. Adding the three regions for each disulfide gives the overall rate constant for that system.

contribution. The absence of a large covalent component explains why a single-parameter substituent analysis (Hammett correlation) works in this case.

The reversible reduction potentials of cobalt compounds **1** and **3** support the above conclusion. If a purely outer-sphere mechanism were operative in the case of the reaction of **1** with disulfides, larger k_1 values should result from the reaction of **3** with disulfides, since **3** is a more powerful reductant. In other words, if both the reaction of **1** with RSSR and **3** with RSSR are assumed to be outer-sphere electron-transfer processes, then the driving force for the $CoCp_2$ reaction should be much larger. In fact, the absolute rate constant values for the reaction of **3** with disulfides are significantly *lower* than those obtained for the reaction of **1** with disulfides. This, along with the strikingly different Marcus plots (Figure 6), supports the operation of an outer-sphere mechanism for **3** and the presence of substantial covalent character (or inner-sphere character) in the transition state of the reaction of **1** with aromatic disulfides.

The effect of solvent was examined for the reaction of **3** with di-*p*-tolyl disulfide and the reaction of **3** with bis[*p*-(trifluoromethyl)phenyl] disulfide. A *P* value of 2.0 for the tolyl reaction indicated that the amount of charge separation in the transition state for this reaction is significant. It is interesting that this value for the sensitivity to solvent polarity is approximately the same as the value found for the reaction of **1** with bis[*p*-(trifluoromethyl)phenyl] disulfide. In both of these reactions, the electrostatic character of the reaction is the clearly the most important factor in the overall rate constant. As the electrostatic character of the reaction becomes even more important (the case in **3** + bis[*p*-(trifluoromethyl)phenyl] disulfide), the sensitivity of the reaction to solvent polarity becomes even greater ($P = 3.9$). Thus, it appears that even the reaction of **3** with disulfides cannot simply be thought of as occurring via the mechanistic extreme of outer-sphere electron-transfer depicted in Scheme 2. Rather, covalent contributions, though minor, still affect the reaction rate. This may explain why the solvent effect is less for the reaction of **3** with bis(*p*-methoxyphenyl) disulfide than for the reaction of **3** with bis[*p*-(trifluoromethyl)phenyl] disulfide.

Conclusions

As shown in eq 3, we have synthesized and fully characterized a series of Ta/Co thiolate complexes from the reaction of paramagnetic **1** with aromatic disulfides. Through a series of kinetic and substituent effect studies, we have found the reaction of **1** with diaryl disulfides to be a relatively facile, associative, bimolecular process. A large steric effect decreasing the reaction rate was induced when the diaryl disulfide used had methyl groups attached at the ortho positions. A Hammett σ/ρ study designed to investigate the distribution of charge in the rate-determining transition state of the reaction of **1** with aromatic disulfides gave a nonlinear correlation. A qualitative Marcus plot clearly showed that the log of the relative rate constants was not linearly related to the peak potential of the disulfide. Both strongly electron-donating and electron-withdrawing groups attached on the aryl rings of the disulfide enhanced the rate relative to the parent diphenyl disulfide.

Application of the *E*- and *C*-based dual-parameter substituent constant analysis successfully fit the data. The reaction was found to be sensitive to both the electrostatic and covalent characteristics of the entering disulfide. The rate-determining transition structure **5** shown in Scheme 1 best explains all of the data. The amount of charge buildup in the transition structure is determined by the incoming disulfide. Electron-withdrawing groups stabilize a large amount of charge separation akin to outer-sphere electron transfer, and electron-donating substituents stabilize a more covalent, concerted process. The *E*- and *C*-based model provides an effective means of analyzing a reaction in which the mechanism changes relatively smoothly as the electronic character of one reactant changes.

The effect of solvent on reaction rate was investigated using the USM-derived quantitative nonspecific solvation analysis model. All substituents examined (excluding *p*-CF_3) exhibited approximately the same solvent effect. This result is consistent with the fine balance between electrostatic and covalent contributions for these substituents. In the reaction of **1** with the strongly electron withdrawing substituted bis[*p*-(trifluoromethyl)phenyl] disulfide, the system becomes much more sensitive to solvent polarity changes. On the basis of the *EC* analysis, this is attributed to the electrostatic contribution being significantly more important than the covalent contribution.

The reaction of cobaltocene (**3**) with aromatic disulfides (expected to proceed by an outer-sphere electron-transfer mechanism) was used as a comparative model reaction. Kinetic, solvent effect, and substituent effect studies confirmed a rate-determining outer-sphere electron-transfer pathway. A linear Hammett σ/ρ correlation indicated that electron-donating groups on the disulfide hamper the reaction rate, while electron-withdrawing substituents enhance it. The absence of a steric effect along with a linear relationship between the log of the relative rate constant and the disulfide peak potential were also consistent with the operation of an outer-sphere single-electron-transfer process. Application of the *E*- and *C*-based dual-parameter substituent constant analysis in this case confirmed that the reaction is sensitive to the electrostatic character of the entering disulfide and relatively insensitive to the covalent characteristics of the incoming disulfide. Use of the USM-derived quantitative solvation analysis in the case of the reaction of **3** with di-*p*-tolyl disulfide gave approximately the same solvent effect as that of the reaction of **1** with bis[*p*-(trifluoromethyl)phenyl] disulfide. This is consistent with the large electrostatic contribution to the rate in both reactions. The reaction of **3** with bis[*p*-(trifluoromethyl)phenyl] disulfide exhibited the most dominant electrostatic contribution and the greatest sensitivity to solvent polarity changes. The difference in solvent effects between *p*-CF_3 and *p*-CH_3 substituents may be attributed to some residual covalent character in the electron-

transfer transition state for this reaction. Although minor, this contribution is still important in the reaction of **3** with diaryl disulfides.

Experimental Section

General Procedure. Unless indicated, all manipulations were carried out under an inert atmosphere in a Vacuum Atmospheres drybox or by using standard Schlenk or vacuum line techniques. Solutions were degassed by sequentially freezing to −196 °C, evacuating under high vacuum, and thawing. This sequence was repeated three times in each case. Glass reaction vessels fitted with ground glass joints and Teflon stopcocks are referred to as bombs.

^{1}H, ^{13}C, and ^{19}F NMR spectra were obtained on either the 300-, 400-, or 500-MHz Fourier transform spectrometers at the University of California, Berkeley (UCB) NMR facility. The 400- and 500-MHz instruments were Bruker AM series spectrometers. Two additional (300- and 400-MHz) instruments were Bruker AMX series spectrometers, while some spectra were recorded on a 500-MHz Bruker DRX series spectrometer.

IR spectra were recorded on a Mattson Galaxy series FT-IR 3000 spectrometer. Mass spectroscopic analyses were obtained at the UCB mass spectrometry facility on AEI MS-12 and Kratos MS-50 mass spectrometers. Elemental analyses were performed by the UCB microanalytical lab. Melting points were recorded for compounds in sealed capillary tubes under nitrogen and are uncorrected.

Unless specified, all reagents were purchased from commercial suppliers and used without subsequent purification. Benzene, toluene, diethyl ether, and pentane were distilled from sodium/benzophenone ketyl under nitrogen. Acetone was dried over 4 Å molecular sieves under nitrogen and subsequently distilled under vacuum. Methylene chloride was distilled from calcium hydride under nitrogen. Benzene-d_6 was vacuum transferred from sodium/benzophenone ketyl. Acetonitrile, methylene-d_2 chloride, and acetonitrile-d_3 were vacuum transferred from calcium hydride. Paramagnetic $Cp_2Ta(\mu\text{-}CH_2)_2CoCp$ (**1**) was prepared according to the literature method.[22] All disulfides were recrystallized from diethyl ether at −30 °C under nitrogen. 2,6-Dimethylphenylsulfenyl chloride was synthesized via the oxidation of the corresponding thiol with chlorine gas dissolved in carbon tetrachloride, a general method for sulfenyl halide preparation.[42] Preparation of this compound by treating the corresponding thioester with thionyl chloride has been reported.[43]

Bis(2,6-dimethylphenyl) Disulfide. In a fume hood, 2,6-dimethylthiophenol (0.22 mL, 1.6 mmol) was dissolved in diethyl ether (15 mL) in a 100-mL Schlenk flask equipped with a magnetic stir bar. The colorless solution was stirred and cooled to 0 °C. A diethyl ether (10 mL) solution of orange 2,6-dimethylphenylsulfenyl chloride (0.29 g, 1.7 mmol) was added, and the mixture turned slightly yellow. The flask was capped with a rubber septum and allowed to stir for 1 h. The volatile materials were removed in vacuo to leave a white residue which was recrystallized from diethyl ether at −30 °C under nitrogen. Bis-(2,6-dimethylphenyl) disulfide (0.383 g, 85% yield) was isolated as white crystals. The ^{1}H and ^{13}C{^{1}H} NMR spectra of this material matched that of bis(2,6-dimethylphenyl) disulfide prepared by alternative routes.[44,45]

$Cp_2Ta(\mu\text{-}CH_2)_2Co(SC_6H_3(CH_3)_2)Cp$ (2a). In a 20-mL vessel equipped with a magnetic stir bar, **1** (0.071 g, 0.15 mmol) was suspended in toluene (5 mL). The yellow suspension was stirred, and a solution of bis(2,6-dimethylphenyl) disulfide (0.0267 g, 0.0973 mmol) in toluene (7 mL) was added dropwise. The mixture was stirred for 18 h during which time it became a homogeneous, dark brown solution. The volatile materials were removed in vacuo, and the residue was washed with pentane (3 × 5 mL). The brown powder left behind was dried in vacuo, dissolved in toluene (7 mL), and layered with pentane (8 mL). After 1 d, the solvents had diffused together and the mixture was cooled to −30 °C. After 18 h, **2a** (0.077 g, 84% yield) was isolated as dark brown platelike crystals, mp 125−127 °C (dec). ^{1}H NMR (CD_2Cl_2): δ 8.99 (d, 2H, J_{H-H} = 8.7 Hz), 7.39 (d, 2H, J_{H-H} = 8.7 Hz), 6.95 (m, 3H), 5.37 (s, 5H), 5.04 (s, 5H), 4.36 (s, 5H), 2.43 (s, 6H). ^{13}C{^{1}H} NMR (CD_2Cl_2): δ 191.0, 190.9, 127.1, 123.2, 119.4, 101.9, 99.0, 87.8, 24.1. Anal. Calcd for $C_{25}H_{28}CoSTa$: C, 50.01; H, 4.70. Found: C, 49.95; H, 4.78.

$Cp_2Ta(\mu\text{-}CH_2)_2Co(SC_6H_4OCH_3)Cp\cdot 0.5\ C_6H_6$ (2b). In a 20-mL vessel equipped with a magnetic stir bar, **1** (0.050 g, 0.11 mmol) was suspended in toluene (6 mL). The yellow suspension was stirred, and a solution of bis(*p*-methoxyphenyl) disulfide (0.021 g, 0.075 mmol) in toluene (6 mL) was added dropwise over 2 min. The mixture was stirred for 6 h during which time it became a homogeneous, red-violet solution. The volatile materials were removed in vacuo, and the residue was washed with cold pentane (4 × 5 mL, −30 °C). The residue was dried in vacuo, dissolved in benzene (10 mL), and layered with pentane (7 mL). After 2 d, **2b** (0.0434 g, 66% yield) was isolated as red-violet crystals, mp 126−130 °C. The amount of benzene solvate was quantified by NMR spectroscopy. ^{1}H NMR (CD_2Cl_2): δ 8.81 (d, 2H, J_{H-H} = 8.4 Hz), 7.38 (d, 2H, J_{H-H} = 8.0 Hz), 7.32 (s, 3H), 6.76 (d, 2H, J_{H-H} = 8.4 Hz), 6.59 (d, 2H, J_{H-H} = 7.6 Hz), 5.33 (s, 5 H), 5.05 (s, 5H), 4.76 (s, 5H), 3.72 (s, 3H). ^{13}C{^{1}H} NMR (CD_2Cl_2): δ 155.9, 139.0, 133.5, 128.7, 117.0, 113.6, 102.7, 99.0, 88.3, 55.6. Anal. Calcd for $C_{27}H_{29}CoOSTa$: C, 50.56; H, 4.56. Found: C, 50.61; H, 4.51.

$Cp_2Ta(\mu\text{-}CH_2)_2Co(SC_6H_4CH_3)Cp$ (2c). In a 20-mL vessel equipped with a magnetic stir bar, **1** (0.0432 g, 0.0933 mmol) was suspended in benzene (10 mL). The yellow suspension was stirred, and a solution of di-*p*-tolyl disulfide (0.0162 g, 0.0657 mmol) in benzene (5 mL) was added dropwise. The mixture was stirred for 8 h, during which time it became a homogeneous, dark purple solution. The volatile materials were removed in vacuo, and the residue was washed with pentane (4 × 5 mL) until the washings were colorless. The red powder left behind was dried in vacuo. The powder was collected as analytically pure **2c** (0.0516 g, 72% yield), mp 140−145 °C. ^{1}H NMR (CD_2Cl_2): δ 8.80 (d, 2H, J_{H-H} = 7.9 Hz), 7.34 (d, 2H, J_{H-H} = 7.9 Hz), 6.77 (m, 4H), 5.32 (s, 5 H), 5.06 (s, 5H), 4.80 (s, 5H), 2.25 (s, 3H). ^{13}C{^{1}H} NMR (CD_2Cl_2): δ 144.7, 132.0, 130.5, 128.4, 116.7, 102.7, 99.0, 88.2, 20.8. IR (KBr): 3111, 2916, 1734, 1655, 1639, 1630, 1595, 1479, 1439, 1257, 1079, 1014, 906, 833, 808 cm^{-1}. Anal. Calcd for $C_{24}H_{26}$-CoSTa: C, 49.16; H 4.47. Found: C, 49.20; H 4.76.

$Cp_2Ta(\mu\text{-}CH_2)_2Co(SC_6H_5)Cp\cdot C_6H_6$ (2d). In a 20-mL vessel equipped with a magnetic stir bar, **1** (0.0965 g, 0.208 mmol) was suspended in benzene (7 mL). The yellow suspension was stirred, and a solution of diphenyl disulfide (0.0318 g, 0.146 mmol) in benzene (8 mL) was added dropwise over 3 min. The mixture was stirred for 3 h, during which time it became a homogeneous, dark purple solution. The volatile materials were removed in vacuo, and the residue was washed with pentane (3 × 4 mL) until the washings were colorless. The solid was dissolved in benzene (2 mL) and layered with pentane (10 mL). After 1 d, **2d** (0.0835 g, 66% yield) was isolated as dark violet crystals, mp 129−132 °C. The amount of benzene solvate was quantified by NMR spectroscopy. ^{1}H NMR (CD_2Cl_2): δ 8.82 (d, 2H, J_{H-H} = 7.8 Hz), 7.48 (d, 2H, J_{H-H} = 8.4 Hz), 7.35 (s, 6H), 6.96 (t, J_{H-H} = 7.8 Hz), 6.82 (m, 1H), 6.78 (d, 2H, J_{H-H} = 8.4 Hz), 5.31 (s, 5H), 5.07 (s, 5H), 4.83 (s, 5H). ^{13}C{^{1}H} NMR (CD_2Cl_2): δ 148.9, 131.7, 128.6, 127.4, 120.7, 116.6, 102.7, 99.0, 88.1. IR (KBr): 3115, 2954, 2914, 1732, 1572, 1452, 1435, 1425, 1263, 1078, 1020, 1011, 901, 841, 831, 822 cm^{-1}. Anal. Calcd for $C_{29}H_{30}CoSTa$: C, 53.55; H 4.65. Found: C, 53.39; H 4.83.

$Cp_2Ta(\mu\text{-}CH_2)_2Co(SC_6H_4CF_3)Cp$ (2f). In a 20-mL vessel equipped with a magnetic stir bar, **1** (0.075 g, 0.16 mmol) was suspended in toluene (10 mL). The yellow suspension was stirred, and a solution of bis[*p*-(trifluoromethyl)phenyl] disulfide (0.0391 g, 0.110 mmol) in toluene (5 mL) was added dropwise over 2 min. The mixture became a brown-orange homogeneous solution over the course of 2 min and was allowed to stir for 18 h. The volatile materials were removed in

(42) Capozzi, G.; Modena, G. In *The Chemistry of the Thiol Group*; Patai, S., Ed.; John Wiley & Sons Ltd: Great Britain, 1974; Vol. 2; p 791.

(43) Cevasco, G.; Novi, M.; Petrillo, G.; Thea, S. *Gazz. Chim. Ital.* **1990**, *120*, 131.

(44) Fujihara, H.; Chiu, J.-J.; Furukawa, N. *Bull. Chem. Soc. Jpn.* **1991**, *64*, 699.

(45) Yamamoto, K.; Yoshida, S.; Nishide, H.; Tsuchida, E. *Bull. Chem. Soc. Jpn.* **1989**, *62*, 3655.

vacuo, and the residue was washed with pentane (5 × 10 mL), followed by cold diethyl ether (10 × 3 mL). The residue was dried in vacuo, dissolved in benzene (6 mL), and layered with pentane (7 mL). After 2 d, **2f** (0.062 g, 60% yield) was isolated as red-violet crystals, mp 134−137 °C. ^{1}H NMR (CD_2Cl_2): δ 8.82 (d, 2H, J_{H-H} = 8.8 Hz), 7.59 (d, 2H, J_{H-H} = 8.0 Hz), 7.17 (d, 2H, J_{H-H} = 8.0 Hz), 6.74 (d, 2H, J_{H-H} = 8.8 Hz), 5.28 (s, 5 H), 5.08 (s, 5H), 4.86 (s, 5H). ^{13}C{^{1}H} NMR (CD_2Cl_2): δ 156.4, 131.1, 127.2, 123.8 (q, J_{C-F} = 3.9 Hz), 116.4, 107.9, 102.8, 99.2, 88.0. ^{19}F NMR (CD_2Cl_2): δ −52.8. Anal Calcd for $C_{24}H_{23}CoF_3STa$: C, 45.01; H, 3.62. Found: C, 44.77; H, 3.65.

[Cp_2Co][$SC_6H_4CF_3$] (4a). In a 20-mL vessel equipped with a magnetic stir bar, **3** (0.065 g, 0.34 mmol) was dissolved in acetonitrile (10 mL). The dark brown solution was stirred, and a solution of bis-[*p*-(trifluoromethyl)phenyl] disulfide (0.062 g, 0.18 mmol) in acetonitrile (5 mL) was added dropwise over 2 min. The mixture turned orange immediately and was allowed to stir for 4 h. The volatile materials were removed in vacuo, and the residue was washed with toluene (3 × 5 mL). The residue was dried in vacuo and dissolved in acetonitrile (5 mL). This solution was then layered with diethyl ether (7 mL). After 1 d at room temperature, the solvents had diffused together. The mixture was cooled to −30 °C. After 1 d at −30 °C, **4a** (0.109 g, 87% yield) was isolated as deep orange needlelike crystals, mp 119−123 °C. ^{1}H NMR (CD_3CN): δ 7.27 (d, 2H, J_{H-H} = 8.0 Hz), 6.95 (d, 2H, J_{H-H} = 8.0 Hz), 5.64 (s, 10H). ^{13}C{^{1}H} NMR (CD_3CN): δ 138.6, 133.1, 130.4, 128.2 (quartet, J_{C-F} = 1.8 Hz) 122.7, 91.1. ^{19}F NMR (CD_2Cl_2): δ −49.0. Anal. Calcd for $C_{17}H_{14}CoF_3S$: C, 45.01; H, 3.62. Found: C, 44.77; H, 3.65. Only one of the cobaltocenium salts **4** was fully characterized; NMR spectral data for the other compounds were similar for all of these salts. The cobaltocenium salts **4** are excellent sources of soluble $[SR]^-$. For example, **4** reacts readily at room temperature with methylene chloride (vide infra).

UV−Visible Kinetics: Reaction of $Cp_2Ta(\mu\text{-}CH_2)_2CoCp$ (1) with Di-*p*-tolyl Disulfide. A stock solution of **1** in methylene chloride ([**2**] = 1.00 × 10^{-3} M) was used in all measurements in the regime in which disulfide was in excess. In each run, a known amount of di-*p*-tolyl disulfide was dissolved in 2.00 mL of methylene chloride. A 1.00-mL aliquot of the disulfide solution was added to a 1.00-mL stock solution of **1**. The solution thus obtained, 0.500 × 10^{-3} M in **2**, was placed in a UV cell fused to a Kontes high-vacuum stopcock. The solution was brought to the appropriate temperature in the temperature control unit of the UV−vis spectrometer, and spectra were recorded at regular intervals so that 30−40 points were collected over 3−6 half-lives of the reaction. The intensity of the absorption at λ = 510 nm (E = 1729 M^{-1} cm^{-1}) was recorded for each spectrum. The data thus obtained were used to plot absorbance vs time. The plot obtained was fit with a first-order exponential growth equation. In all runs the correlation coefficient R was greater than 0.999.

This procedure was repeated using acetonitrile, diethyl ether, and acetone solvents, as well as with other disulfides in methylene chloride. In the kinetic measurements of the reaction of excess **1** with di-*p*-tolyl disulfide, a similar procedure was followed except that the concentration of excess **1** was ≥9 times (18 Normal times) the concentration of disulfide. In some cases, the reaction was too rapid to measure using standard techniques. In these cases, an anaerobic stopped flow apparatus connected to the UV−vis spectrometer was used (vide infra).

Under the flooding regime in which **1** is in excess, a different analysis of the correct rate law must be derived. The appearance of **2c** is related to the disappearance of di-*p*-tolyl disulfide by eq 9. This expression leads to eq 10, where [di-*p*-tolyl disulfide]$_i$ is the initial concentration of di-*p*-tolyl disulfide:

$$d[\mathbf{2c}]/dt = -2(d[\text{di-}p\text{-tolyl sulfide}]/dt) \quad (9)$$

$$[\text{di-}p\text{-tolyl sulfide}] = [\text{di-}p\text{-tolyl sulfide}]_i - 0.5[\mathbf{2c}] \quad (10)$$

This can be substituted into the rate law (eq 4), when, under pseudo-first-order conditions, k_{obs} is equal to $2k_1[\mathbf{1}]$. Integrating the substituted equation leads to the desired exponential function (eq 11) which can also be expressed in its logarithmic form (eq 12).

$$[\text{di-}p\text{-tolyl sulfide}]_i\{1 - [0.5\exp(-0.5k_{obs}t)]\} = [\mathbf{2c}] \quad (11)$$

$$-2\ln\{1 - [0.5([\mathbf{2c}]/[\text{di-}p\text{-tolyl sulfide}]_i)]\} = k_{obs}t \quad (12)$$

UV−Visible Kinetics: Reaction of $CoCp_2$ (3) with Aromatic Disulfides. A stock solution of **3** in methylene chloride ([**3**] = 1.09 × 10^{-3} M) was used in all measurements. In each run, a known amount of disulfide was dissolved in 2.00 mL of methylene chloride. A 1.00-mL aliquot of the disulfide solution was added to a 1.00-mL stock solution of **3**. The solution thus obtained, 0.505 × 10^{-3} M in **3**, was placed in a UV cell fused to a Kontes high-vacuum stopcock. The solution was brought to the appropriate temperature in the temperature control unit of the UV−vis spectrometer, and spectra were recorded at regular intervals so that 30−40 points were collected over 3−6 half-lives of the reaction. The intensity of the absorption at λ = 378 nm was recorded for each spectrum. The data thus obtained were used to plot absorbance vs time. The plot obtained was fit with a first-order exponential decay equation. In all runs the correlation coefficient R was greater than 0.99.

This procedure was repeated using acetonitrile and acetone solvents, as well as with other disulfides in methylene chloride. In some cases, the reaction was too rapid to measure using standard techniques. In these cases, an anaerobic stopped flow apparatus connected to the UV−vis spectrometer was used (vide infra).

Control experiments were carried out to investigate the possible reactivity of the starting materials and products toward methylene chloride solvent. The reaction of **3** with methylene chloride is too slow at 15 °C to affect the data. This was shown by a UV−vis experiment in which a CH_2Cl_2 solution of **3** was monitored over 48 h at 15 °C and showed essentially no spectral change. The reaction of thiolate anion with methylene chloride is a fast process, but again does not affect this study as the disappearance of **3** was measured (not the appearance of **4**). The data showed excellent pseudo-first-order kinetic behavior (see Supporting Information).

UV−Visible Kinetics: Stopped-Flow Experiments. These experiments were performed using a Hi-Tech Scientific SFA-20 rapid kinetics stopped-flow accessory with an anaerobic kit connected to an Hewlett-Packard 8453 UV−vis spectrometer. The accessory was maintained under a nitrogen or argon atmosphere, and the flow circuit itself was also purged with nitrogen or argon before use. Prior to the introduction of the reagents, the flow circuit was flushed with 40 mL of dry, oxygen-free solvent. Both decay of starting material and growth of product were monitored. The wavelength maxima monitored were verified in standard experiments where spectra before and after a solid reagent was added were taken.

In a typical experiment, a stock solution of **1** or **3** was prepared as described in the standard experiments. One gastight reservoir syringe was loaded with approximately 10 mL of this solution, and the other was loaded with 10 mL of a solution containing a 10-fold excess of the examined disulfide. Ca. 5 mL of each solution was flowed through the flow circuit to the waste syringe, and then the flow was quickly opened to the "stop", triggering data acquisition. The average rate constant at 15 °C was determined by averaging rate constants from at least five (typically 10) "shots". Rates of decay of the starting material matched rates of growth of the product in all cases. Data were fit using the same methods as for the standard experiments, and the quality of the fits was similar.

***E*- and *C*-Based Dual-Parameter Substituent Constant Calculations.** The log of the measured rate constant ($\Delta\chi^X$) are fit to eq 5 using the ΔE^X and ΔC^X parameters derived for each para substituent.[29] An equation for each measurement is written, and the simultaneous equations derived are solved for d^E, d^C, and $\Delta\chi^H$ using a simple multiple regression program. In the case of the parent phenyl substituent, $\Delta\chi^H$ was entered as an X-substituent with $\Delta E^H = \Delta C^H = 0$. The value of the measured property (in this case, the second-order rate constant) for the X substituent is symbolized by $\Delta\chi^X$, while the second-order rate constant for diphenyl disulfide (X = H) is symbolized by $\Delta\chi^H$. For all reactions, the R^2 value for these fits ranged from 0.9999 to 0.82; however, similar trends were observed between fits of varying qualities (vide supra). Multicollinearity was, at worst, a mild problem.

Electrochemical Measurements. All measurements were carried out in an argon-filled drybox using a BAS 100A electrochemical analyzer. Samples were prepared such that the solution was as close

as possible to 5 mM in substrate and exactly 0.1 M tetrabutylammonium hexafluorophosphate in acetonitrile. The configuration of the cell consisted of three electrodes: the working electrode (platinum), a platinum wire counter electrode, and a $Ag/AgNO_3$ (0.01 M) nonaqueous reference electrode. Potentials were recorded relative to the silver electrode which was calibrated using ferrocene.[46]

X-ray Crystallographic Analysis of $Cp_2Ta(\mu\text{-}CH_2)_2Co(SC_6H_3(CH_3)_2)Cp$ (2a). Dark brown platelike crystals of the compound were obtained from toluene/pentane diffusion as described above. A fragment of one of these crystals was mounted on a glass fiber using Paratone N hydrocarbon oil. The crystal was transferred to a Siemens SMART diffractometer,[47] centered in the beam, and cooled to −120 °C by a nitrogen-flow apparatus.

After data collection, the data were integrated using the Siemens program SAINT to a maximum 2θ of 50.9° (92% coverage). Corrections were made for Lorentz and polarization effects, but no correction for decay was necessary. The data were corrected for absorption by an empirical correction based on multiple measurements of symmetry equivalent and redundant reflections using the Siemens program XPREP. The 9228 integrated and corrected reflections were averaged to yield 2075 unique reflections for solution.

The structure was solved by direct methods and expanded using Fourier techniques. Data collection and refinement parameters can be found in Table 1. All non-hydrogen atoms were refined anisotropically. Hydrogen atoms were included in predicted positions but not refined. The positional and thermal parameters for the non-hydrogen atoms are given in the Supporting Information (Table S-1), while selected intramolecular distances and angles are given in Tables 2 and 3, respectively.

(46) Schumann, H. *J. Organomet. Chem.* **1985**, *290*, C34.

(47) All calculations were performed using the teXsan crystallographic software package of Molecular Structure Corp.

Acknowledgment. We dedicate this paper to the memory of Prof. Russell S. Drago, who provided us with much helpful advice on the application of the *E*- and *C*-based dual-parameter substituent constant model and the use of the USM-derived quantitative, nonspecific solvation model during the course of this work. We thank Prof. Warren P. Giering and Dr. Steven J. Skoog for helpful discussions on QUALE and Marcus theory, respectively. We also acknowledge Dr. F. J. Hollander, director of the UC-Berkeley X-ray diffraction facility (CHEXRAY), for determination of the X-ray structure and Brandon Weldon and Prof. James McCusker for assistance with the voltammetry experiments. We are grateful for support of this work from the National Science Foundation (Grant No. CHE-9633374).

Supporting Information Available: Representative kinetic data for the reaction of **1** with disulfides, representative kinetic data for the reaction of **3** with disulfides, and positional parameters and their estimated standard deviations for $Cp_2Ta(\mu\text{-}CH_2)_2Co(SC_6H_3(CH_3)_2)Cp$ (**2a**) (7 pages, print/PDF). See any current masthead page for ordering information and Web access instructions.

JA980878E